

Radiative transfer models (RTMs) for field phenotyping inversion of rice based on UAV hyperspectral remote sensing

Yu Fenghua¹, Xu Tongyu^{1,2*}, Du Wen¹, Ma Hang¹, Zhang Guosheng¹, Chen Chunling^{1,2}

(1. College of Information and Electrical Engineering, Shenyang Agricultural University, Shenyang 110866, China;

2. Liaoning Engineering Research Center for Information Technology in Agriculture, Shenyang 110866, China)

Abstract: The nondestructive and rapid acquisition of rice field phenotyping information is very important for the precision management of the rice growth process. In this research, the phenotyping information LAI (leaf area index), leaf chlorophyll content (C_{ab}), canopy water content (C_w), and dry matter content (C_{dm}) of rice was inverted based on the hyperspectral remote sensing technology of an unmanned aerial vehicle (UAV). The improved Sobol global sensitivity analysis (GSA) method was used to analyze the input parameters of the PROSAIL model in the spectral band range of 400-1100 nm, which was obtained by hyperspectral remote sensing by the UAV. The results show that C_{ab} mainly affects the spectrum on 400-780 nm band, C_{dm} on 760-1000 nm band, C_w on 900-1100 nm band, and LAI on the entire band. The hyperspectral data of the 400-1100 nm band of the rice canopy were acquired by using the M600 UAV remote sensing platform, and the radiance calibration was converted to the canopy emission rate. In combination with the PROSAIL model, the particle swarm optimization algorithm was used to retrieve rice phenotyping information by constructing the cost function. The results showed the following: (1) an accuracy of $R^2=0.833$ and RMSE=0.0969, where RMSE denotes root-mean-square error, was obtained for C_{ab} retrieval; $R^2=0.816$ and RMSE=0.1012 for LAI inversion; $R^2=0.793$ and RMSE=0.1084 for C_{dm} ; and $R^2=0.665$ and RMSE=0.1325 for C_w . The C_w inversion accuracy was not particularly high. (2) The same band will be affected by multiple parameters at the same time. (3) This study adopted the rice phenotyping information inversion method to expand the rice hyperspectral information acquisition field of a UAV based on the phenotypic information retrieval accuracy using a high level of field spectral radiometric accuracy. The inversion method featured a good mechanism, high universality, and easy implementation, which can provide a reference for nondestructive and rapid inversion of rice biochemical parameters using UAV hyperspectral remote sensing.

Keywords: UAV, rice phenotyping inversion, hyperspectral remote sensing, PROSAIL model, global sensitivity analysis, precision management

DOI: 10.25165/j.ijabe.20171004.3076

Citation: Yu F H, Xu T Y, Du W, Ma H, Zhang G S, Chen C L. Radiative transfer models (RTMs) for field phenotyping inversion of rice based on UAV hyperspectral remote sensing. Int J Agric & Biol Eng, 2017; 10(4): 150–157.

1 Introduction

Rice is the world's most important staple crop for

human survival and development. With a substantial increase in the world's population and the demand for food, the modernization and accurate production of rice is very important^[1]. Detection and acquisition of rice growth information is an important role in guiding the growth of rice and increasing yield. The acquisition of traditional rice information is facilitated through the laboratory chemical analysis method, but field sample collection and determination also consume time, manpower, and material resources, and are not conducive to the timely monitoring of rice growth. Therefore, how to introduce newer and modern technologies to carry out fast, nondestructive, large-area synchronous observation and accurately obtain rice growth information, and effectively guide rice production, has become a major

Received date: 2016-12-02 **Accepted date:** 2017-04-18

Biographies: **Yu Fenghua**, PhD candidate, research interest: agricultural remote sensing, Email: adan@syau.edu.cn; **Du Wen**, PhD candidate, research interest: agricultural remote sensing, Email: duwen@syau.edu.cn; **Ma Hang**, Master student, research interest: agricultural remote sensing, Email: 1057934411@qq.com; **Zhang Guosheng**, Master student, research interest: agricultural remote sensing, Email: 287063310@qq.com; **Chen Chunling**, PhD, Associate Professor, research interest: agricultural remote sensing, Email: 342082281@qq.com.

***Corresponding author:** **Xu Tongyu**, PhD, Professor, research interest: agricultural remote sensing, College of Information and Electrical Engineering, Shenyang Agricultural University, Shenyang 110866, China. Email: yatongmu@163.com.

agricultural topic both domestically in China and internationally. Unmanned aerial vehicle (UAV) remote sensing technology is a type of detection technology that was a product of the development of space and computer technology. The ability to apply rapid, nondestructive, large-area synchronous detection technology to the collection of rice-growing and rice-growth information, to obtain rice-growth status, has important significance to guiding the precise informatization of rice production^[2,3]. At present, UAV remote sensing technology is a hot research field, and it has been widely used to monitor the dynamic change of farmland, forestry, facilities, and other resources by analyzing the remote sensing data collected by UAVs. A large field of rice-yield estimation by remote sensing, along with pest monitoring and an agricultural remote sensing monitoring information system, has been established. The development and application of UAV and remote sensing technology has made rice production and research transition from the use of traditional methods to a new stage of quantitative precision agriculture^[4].

A UAV platform equipped with satellite remote sensing can obtain more abundant agricultural remote sensing data, with better precision and greater dimensional precision than traditional satellite remote sensing. However, since the micro-UAV platform is directly involved in the data collection process, it may itself have a certain impact on the data collection. Therefore, effectively maximizing UAV remote sensing data acquisition and agricultural agronomic parameter inversion accuracy is the key to using the micro-UAV remote sensing research platform for agriculture^[5].

Calderón et al.^[6] used Ciganda and other near-infrared reflectance spectroscopy techniques to establish the relationship between the maize leaf and canopy, and thereby the chlorophyll content of maize leaves was retrieved. By obtaining the canopy spectral information of wheat, Atzberge was able to obtain a better model accuracy ($R^2=0.82$) using partial least-squares regression (PLS) to establish the NDVI and canopy chlorophyll models^[7,8]. Swain^[9] used UAV remote sensing inversion to determine rice yield and total biomass. NDVI has been used for regression analysis in the young

panicle differentiation stage to estimate rice yield and total biomass, and in the fitting the R^2 accuracy of the model was 0.728 and 0.760, respectively. These results show that using high-resolution remote sensing data acquired by a micro-UAV remote sensing system to determine the yield and biomass inversion of a rice-growing area over a good range is viable, and, moreover, reduces the level of error introduced by satellite remote sensing. In some studies, some scholars have used the GNDVI vegetation index to retrieve the LAI, and the accuracy of the inversion model ($R^2=0.65$) can also be used to detect the LAI via UAV remote sensing. A UAV equipped with a variety of spectrometers for remote sensing monitoring of rice, can obtain spectral information of a series of corresponding crop, agronomic parameter inversion, but including some crop spectral analysis strains with high, plant type, internal temperature information is not the optimal way^[10-13].

In the research described in this paper, a UAV equipped with a hyperspectral imaging camera was used to gather rice canopy spectral information. The sensitive band of PROSAIL input parameters was obtained by global sensitivity analysis (GSA), using the particle swarm optimization (PSO) algorithm of the PROSAIL model, the PROSAIL simulation model of rice canopy spectral information, and the actual measured canopy spectral information in order to obtain the smallest difference in rice the chlorophyll concentration (C_{ab}), the equivalent water thickness (C_w), the dry matter content (C_{dm}), and the leaf area index (LAI), comprising the four parameters for determining the growth response of rice.

2 Materials and methods

2.1 Testing site

The experiment was conducted in the rice-breeding field at Shenyang Agricultural University (41°49'N, 123°33'E; altitude 65 m) in Shenyang, Liaoning Province, China. The Japonica rice (Shendao-529) cultivar was transplanted on May 29, 2016. Shendao-529 is suitable for cultivation in East and North Liaoning Province, where the growth period is 148-150 d. The rice experiment field is shown in Figure 1.



Figure 1 Test site: Japonica rice experiment field at Shenyang Agricultural University, 2016

2.2 Instruments and equipment

A hyperspectral imaging camera (Gaiasky-mini) equipped with an incident light sensor (Dualix Spectral Imaging, Inc., China) is used to collect the remote sensing images of the Japonica rice canopy (Figure 2). There are 256 channels in the hyperspectral camera. The spectral range of the hyperspectral imager is 400-1100 nm and its spectral resolution is 3.5 nm. The imaging method of the spectrometer is built-in push broom. The images were acquired with 16-bit radiometric resolution^[14].



Figure 2 UAV-M600 and Gaiasky-mini hyperspectral imaging camera

The platform for hyperspectral image acquisition is a six-rotor UAV (M600, DJI, China). The UAV can lift 6.5 kg and has a flight time of approximately 20 min. In order to eliminate the effects of vibration in the spectral image acquisition process, the UAV was equipped with a RONIN-MX attitude control system.

2.3 Hyperspectral image and rice sample collection

Hyperspectral images of Japonica rice were collected by the airborne acquisition system between 11:30 and 13:30 on July 28, 2016. The scene of the experiment is

shown in Figure 3. The UAV flew at an altitude of 50 m above the rice canopy. After hyperspectral image collection, 36 Japonica rice leaves were collected from the canopy in an area measuring 1 m² of each experimental plot and stored immediately in refrigerated containers for biophysical parameter analysis (C_{ab} , C_w , C_{dm} , and LAI).



Figure 3 Scene of experiment

2.4 Japonica rice biophysical parameter collection

2.4.1 C_w and C_{dm} measurement of rice leaves

In the laboratory, the fresh weight and area of rice leaves were measured. Rice leaf samples were cleaned and immediately placed into a 105°C oven for 30 min to inactivate enzymes. The rice leaf samples were then dried at 65°C for 72 h or more until the quality of rice leaves was consistent^[15-17]. The quality criterion was C_{dm} . The EWT Equation is:

$$CW = (LFWC - LDWC) / LA \quad (1)$$

where, LFWC represents the quality of fresh leaves of Japonica rice and LDWC and LA the quality of dried leaves of Japonica rice and the total area of Japonica rice samples, respectively.

2.4.2 C_{ab} measurement of rice leaves

Japonica rice samples were taken from a homogenized triturate prepared from 36 experimental plots for each analysis, depending on the randomness of the sampling. Pigment extraction was performed with N-dimethylformamide, and the chlorophyll fraction was purified and the lipid compounds and carotenes removed by liquid-liquid extraction using hexane. All analyses

were performed in triplicate under a green light. The pigments were separated by reverse-phase HPLC using a Hewlett-Packard HP 1100 liquid chromatograph. Separation was performed using an elution gradient with the mobile phases: water/ion pair reagent/methanol (1/1/8, v/v/v) and methanol/acetone (1/1, v/v). The ion pair reagent was 0.05 M tetrabutylammonium and 1 M ammonium acetate in water^[18-20]. Sequential detection was performed with a photodiode array detector at 410 nm, 430 nm, 450 nm and 666 nm, respectively. Data were collected and processed with a LC HP ChemStation (Rev.A.05.04). Pigments were identified by co-chromatography with authentic samples and from their spectral characteristics.

2.4.3 LAI measurement of rice leaves

LAI measurement of rice leaves was performed using a pair of LAI-2200C sensors. Accurate measurement of rice canopy transmission requires simultaneous measurements of sky brightness to be taken above (A readings) and below (B readings) the canopy, while viewing the same region of sky^[21]. The height of the canopy in our study required all of the A readings to be obtained using a sensor located in one of the identified clearings. The sensors were matched using the recommended method and synchronized to GPS time at the start of every time period. The reference sensor was placed on a leveled 2.7 m high tripod and set to obtain A readings every 30 s. All clearings provided unobstructed views of the sky, but 180° view caps were fitted to both sensors to exclude the sun and operator from view.

2.5 PROSAIL models

The PROSAIL model, coupled with the PROSPECT and SAIL models, is one of the most widely used radiative transfer models, and it is often used to invert biochemical parameters^[22]. The PROSPECT model is based on leaf scale, and can be used to simulate the reflectivity and transmittance of leaf blades. The SAIL model uses the vegetation canopy as the scale. It takes the output of the PROSPECT model as its input variable, along with leaf distribution function, solar zenith angle, soil background and other factors. Therefore, the PROSAIL model can be used to establish the relationship

between the plant canopy spectrum and the LAI, the concentration of biochemical substances in leaves, and the quantitative relationship between soils. The main input variables are shown in Table 1.

Table 1 Partial input parameters of PROSAIL model

Model	Parameter	Meaning	Range of values
PROSPECT	N	leaf structure parameter	1-4
	$C_{ab}/\mu\text{g}\cdot\text{cm}^{-2}$	chlorophyll concentration	20-80
	$C_{ar}/\mu\text{g}\cdot\text{cm}^{-2}$	carotenoid concentration	4-17
	$C_m/\text{g}\cdot\text{cm}^{-2}$	dry matter content	0.002-2.00
	C_w/cm	equivalent water thickness	0.0005-0.04
SAIL	LAI	leaf area index	1-5
	ALA/(°)	average leaf angle	20-50
	S_L	hot spot	0.01-1
	Skyl	sky diffuse reflection ratio	0.01-0.4
	tto/(°)	observed zenith angle	-50-50
	tts/(°)	solar zenith angle	-50-50

2.6 Global sensitivity analysis

PROSAIL models vary in design, complexity, number of input variables, and processing speed. Not all PROSAIL input variables play an equally important role; they are also spectrally dependent. For the larger majority of remote sensing applications there is no need to vary all of the variables. Global sensitivity analysis (GSA) techniques, which quantify the relative importance of each input parameter to PROSAIL outputs, can help set safe default values for those less influential input parameters. GSA can greatly simplify model calibration by enabling the most influential parameters to be targeted for data acquisition and refinement^[23].

Sobol is the most popular variance-based method for GSA. This modification has been demonstrated to be effective in identifying the so-called Sobol sensitivity indices. These indices quantify both the main sensitivity effects (first-order effects) (the contribution to the variance of the PROSAIL output by each input variable) and total sensitivity effects (the first-order effect plus interactions with other input variables) of the input variables. Formally, given a model $Y = f(X)$, where Y is the model output, $X = (X_1, X_2, \dots, X_k)$ is the input parameter vector. A variance decomposition of f suggested by Sobol is:

$$V(Y) = \sum_{i=1}^k V_i + \sum_{i=1}^k \sum_{j=i+1}^k V_{ij} \dots + v_{1, \dots, k} \quad (2)$$

where, X is rescaled to a k -dimensional unit hypercube Ω^k ,

$\Omega^k = |X|_{0 \leq X_i \leq 1, i=1, \dots, k}$; $V(Y)$ is the total unconditional variance; V_i is the partial variance or “main effect” of X_i on Y and is given by $V_i = V[E(Y|X_i)]$; and V_{ij} is the joint impact of X_i and X_j on the total variance minus their first-order effects. Here, the first-order sensitivity index S_i and total effect sensitivity index S_{Ti} are:

$$S_i = \frac{V_i}{V(Y)} = \frac{V[E(Y|X_i)]}{V(Y)} \quad (3)$$

$$S_{Ti} = S_i + \sum_{j \neq i} S_{ij} + \dots = \frac{E[V(Y|X_{-i})]}{V(Y)} \quad (4)$$

2.7 Modeling and model evaluation

2.7.1 Hyperspectral data assimilation

In this study, the PSO algorithm was used to optimize the differences between the hyperspectral observations of the rice canopy and the PROSAIL simulation, and to minimize the difference between the simulated and observed values^[24]. The PSO algorithm is simple and easy to apply and, using it, the solution of the problem to be optimized is represented by the position coordinates of the particle, and the current optimal solution (the optimal value) and the current optimal solution of the entire particle population are tracked by the particle^[25].

2.7.2 Model evaluation

The model’s performance was mainly evaluated by the following indices: the correlation coefficients of the calibration (R^2) and the root-mean-square error (RMSE). The best model should have a maximum value of R^2 and a minimum value of the RMSE.

3 Results and discussion

3.1 GSA reflectance results

Five thousand subsamples were used for the GSA. Since its efficiency is relatively slow, it takes 1258 s to analyze the four input parameters (LAI, C_w , C_{ab} and C_{dm}) of the PROSAIL model. The Sobol total order sensitivity index (S_{Ti}) results for the PROSAIL model across the 400-1100 nm region are shown in Figure 4. Despite the large number of PROSAIL input variables, some variables can be obtained directly. Hence, the majority of variables related to micrometeorology and plant physiology have no impact on reflectance. Variables that can be measured directly include hotspot, soil reflectance and leaf structural parameters.

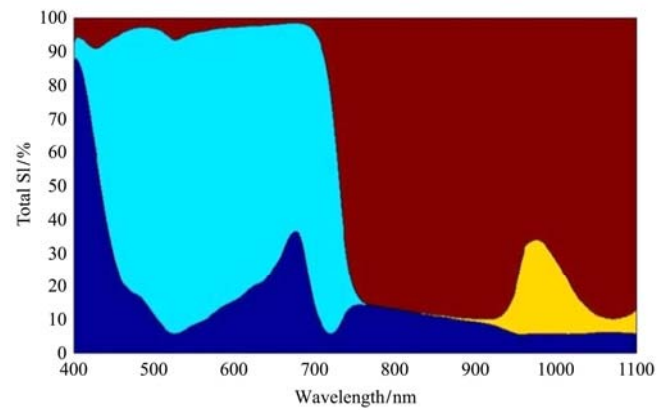


Figure 4 GSA total sensitivity index (S_{Ti}) for PROSAIL reflectance

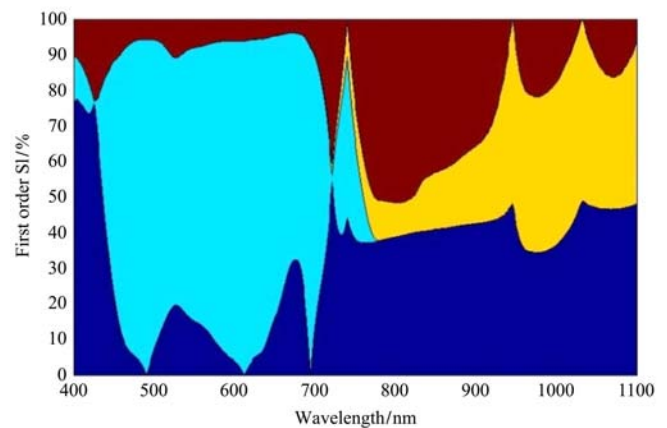


Figure 5 GSA first-order sensitivity index (S_i) for PROSAIL reflectance

As can be seen from Figures 4 and 5, the total sensitivity of the main parameters is different in different wave bands. The canopy reflectance at 400-750 nm was mainly affected by the chlorophyll content, and the total sensitivity of the chlorophyll content to the canopy reflectance was approximately 80%. Almost all of the vegetation indices related to chlorophyll retrieval are within this range. The C_w only affects the spectral band over 800 nm. In the near-infrared (NIR) band of 800-1100 nm, C_w , C_{dm} , and LAI are the three most important parameters affecting the canopy reflectance, and the total sensitivity of the three parameters is approximately 95%. For the LAI and C_{dm} , the spectrum is affected within the range of 400-1100 nm.

3.2 Japonica rice biophysical variable retrieval

Figure 6 shows the average R^2 performance of the PSO methods over 10 runs against validation data. The dashed line represents the R^2 accuracy of the full reference training data set containing 36 samples. Table 2 shows the accuracy of the four parameters of the

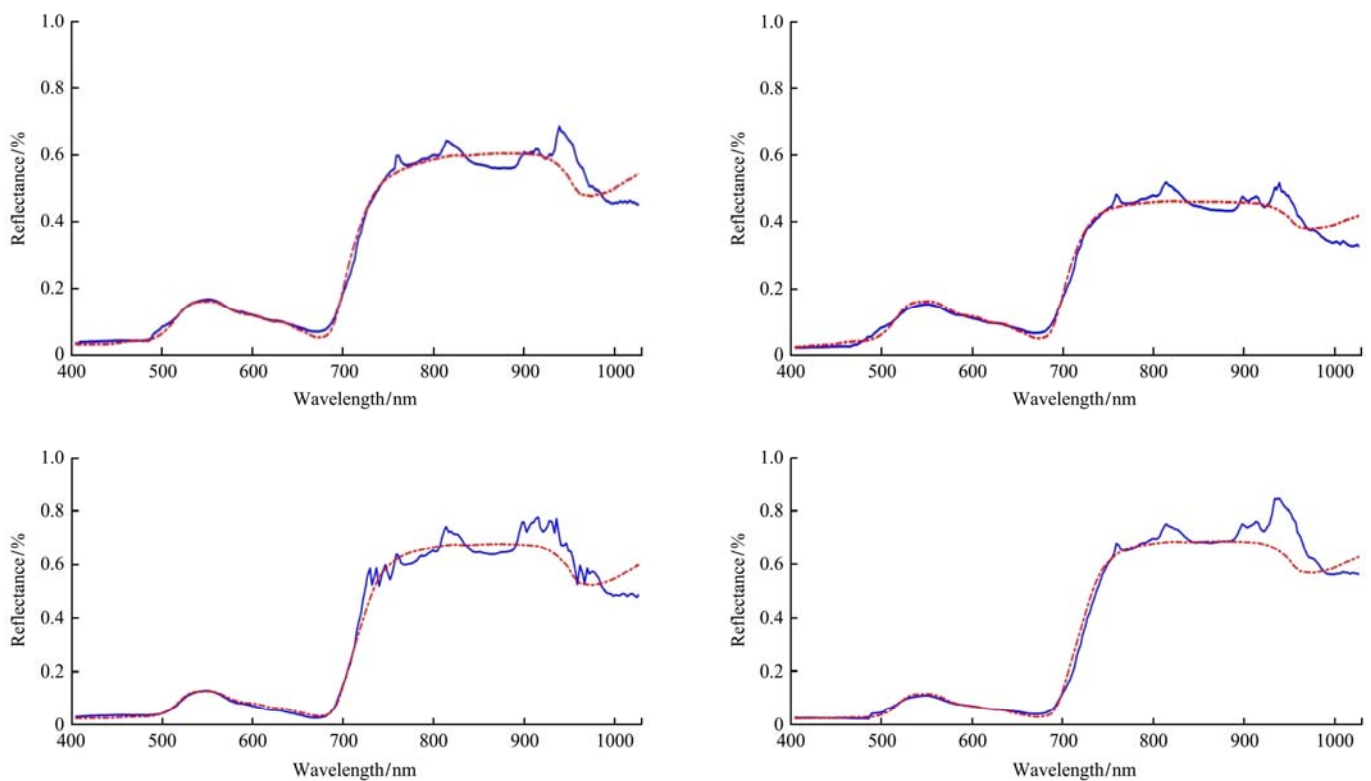
PROSAIL model.

Table 2 Accuracy of the four PROSAIL model parameters

Biophysical variable	R^2	RMSE
LAI	0.816	0.1012
C_w	0.665	0.1325
C_{dm}	0.793	0.1084
C_{ab}	0.833	0.0969

From the Table 2, it is seen that the accuracy of chlorophyll is the best ($R^2=0.833$, $RMSE=0.0969$), which is mainly because the main chlorophyll sensitive band is between 450-750 nm, and the boundary noise of the hyperspectral image of the band in the range 400-1100 nm between the two bands is relatively large, and

has a low signal-to-noise (SNR) ratio, which affects the accuracy of data inversion. When the chlorophyll sensitive band is in the central part of the entire band, the SNR of the hyperspectral remote sensing data is better. The accuracy of C_w is the worst because the sensitive band of water is below 800 nm, and the SNR of the hyperspectral information of the rice canopy at 800-1100 nm is low, which affected the assimilation effect of C_w . The change of LAI and C_{dm} affects the whole band in the range 400-1100 nm, and there is no obvious characteristic band, so the accuracy of inversion effect is greatly affected by other parameters.



Red line: PSO Simulation of the spectral curve. Blue line: The actual measured spectral curve.

Figure 6 Simulated and actual spectral curves after assimilation by PSO algorithm

4 Discussion

Low-altitude hyperspectral remote sensing of Japonica rice by a UAV has the advantages of high efficiency, high image resolution, low cost, and the ability to obtain multiscale and temporal ground remote sensing data. It provides us with a more efficient technique for real-time monitoring of the rice field. Rice is the most important food crop in the world and the leaves in its canopy are more complex. The different distribution, different angles, and different nutrition of

rice leaves will affect the canopy spectral information. In this study, a multirotor UAV was used to obtain hyperspectral information on the rice canopy, and a DN value of 400-1100 nm was converted to the reflectivity by radiometric calibration. However, due to the fact that the environment of the test field is more complex, especially due to changes in light, wind and other factors, calibration errors will occur, which will affect the subsequent data inversion. In this study, black and white cloth was used for radiometric calibration in the field. In order to maximize the consistency of the data, a

radiometric calibration was performed every 5 min.

The hyperspectral remote sensing data collected by the UAV was mainly used for accurate retrieval of the input biophysical parameters of the PROSAIL model. Since the PROSAIL model is complex, a model parameter sensitivity analysis was performed to quantitatively evaluate the influence of each input parameter on the output results. Determining the main effect of different band parameters is the goal of an effective application. In this study, we used GSA to analyze the input parameters of the PROSAIL model. Sensitivity analysis methods can be divided into local and global types. Local sensitivity analysis was carried out within the range of single parameter variation, and the effect of coupling between parameters is neglected, which is difficult to apply in the study of a complex nonlinear model. GSA is used to analyze the changes over the entire range of parameters, and considering the influence of the coupling between different parameters on the output of the model, GSA is very suitable for a complex nonlinear model, and is thus widely used. The PROSAIL model showed that images in the range 400-1100 nm were affected by multiple factors at the same time. The process of this research, through sensitivity analysis, showed that any one band is affected by many variables, so pathological inversion is carried out; that is, different parameters corresponding to the same spectral curve are combined. The data assimilation method was used in this research, and although it was relatively easy to achieve, to reduce the problem of pathological inversion, traditional knowledge from agricultural experience was needed as well.

In this experiment, a manually selected region of interest was used from the remote sensing image in ENVI, which had a negative effect on obtaining better prediction accuracy and fast extraction of spectral information. This is a key issue that needs to be addressed in future studies.

5 Conclusions

Our studies demonstrated that using UAV hyperspectral remote sensing technology combined with the PROSAIL model was able to retrieve the physiological parameters

of rice. The rice canopy hyperspectral data in the range 400-1100 nm were acquired using the M600 UAV remote sensing platform, and the radiance calibration was converted to the canopy emission rate. In combination with the PROSAIL model, the PSO algorithm was used to retrieve rice phenotyping information by constructing the cost function. The results showed the following:

(1) The C_{ab} retrieval accuracy was $R^2=0.833$ and $RMSE=0.0969$, the LAI inversion accuracy was $R^2=0.816$ and $RMSE=0.1012$, the C_{dm} inversion accuracy of was $R^2=0.793$ and $RMSE=0.1084$, and the C_w inversion accuracy was $R^2=0.665$ and $RMSE=0.1325$. As the hyperspectral band in this study used 1000 nm or larger noise, the C_w inversion accuracy was not particularly high.

(2) Because the same band is affected by multiple parameters at the same time, the problem of inversion of phenotyping information occurs when using this method.

(3) This study adopted a rice phenotyping information inversion method to acquire rice hyperspectral information by a UAV based on the phenotypic information retrieval accuracy achieved owing to the high field spectral radiometric accuracy. In this study, UAV remote sensing and the PROSAIL model were combined to invert the phenotyping information of a rice field, which comprised a good mechanism, high universality, and easy implementation. This study provides a theoretical basis for nondestructive and rapid inversion of rice biochemical parameters using UAV hyperspectral remote sensing.

Acknowledgements

The authors gratefully acknowledge the support of the National Key Research and Development Plan of China (Grant No. 2016YFD020060307), Key Project of Education Department of Liaoning province (LSNZD201605).

[References]

- [1] Yu F H, Xu T Y, Cao Y L, Yang G J, Du W, Wang S. Models for estimating the leaf NDVI of japonica rice on a canopy scale by combining canopy NDVI and multisource environmental data in Northeast China. Int J Agric & Biol

- Eng, 2016; 9(5): 132–142.
- [2] Li F, Victor A, Zhao H, Zhao Y J, Cui X F. PLSR-based airborne hyperspectral remote sensing retrieval of leaf nitrogen content in potato fields. *Chinese Journal of Agrometeorology*, 2014; 35(3): 338–343. (in Chinese)
- [3] Zang Y, Gu X Y, Zhou Z Y, Luo X W, Zang Y, Qi X Y, et al. Review of tensairity and its applications in agricultural aviation. *Int J Agric & Biol Eng*, 2016; 9(3): 1-14.
- [4] Gutierrez M. Effect of leaf and spike morphological traits on the relationship between spectral reflectance indices and yield in wheat. *International Journal of Remote Sensing*, 2015; 36(3): 701–718.
- [5] Wu B F, Gommers R, Zhang M, Zeng H W, Yan N N, Zou W T, et al. Global crop monitoring: a satellite-based hierarchical approach. *Remote Sensing*, 2015; 7(4): 3907–3933.
- [6] Calderón R, Navas-Cortés J A, Lucena C, Zarco-Tejada P J. High-resolution airborne hyperspectral and thermal imagery for early detection of *Verticillium* wilt of olive using fluorescence, temperature and narrow-band spectral indices. *Remote Sensing of Environment*, 2013; 139(23): 231–245.
- [7] Huang Y, Thomson S J, Brand H J, Reddy K N. Development of low-altitude remote sensing systems for crop production management. *Int J Agric & Biol Eng*, 2016; 9(4): 1–11.
- [8] Zhang P, Deng L, Lyu Q, He S L, Yi S L, Liu Y D, et al. Effects of citrus tree-shape and spraying height of small unmanned aerial vehicle on droplet distribution. *Int J Agric & Biol Eng*, 2016; 9(4): 45–52.
- [9] Chunhua Z, John M. The application of small unmanned aerial systems for precision agriculture: a review. *Precision Agriculture*, 2012; 12(13): 693-712.
- [10] Xue X Y, Tu K, Qin W C, Lan Y B, Zhang H H. Drift and deposition of ultra-low altitude and low volume application in paddy field. *Int J Agric & Biol Eng*, 2014; 7(4): 23–28.
- [11] Zhou Y, Hao J P, Zheng J. The development and research trend of beam string structure exploration. *Industrial Building*, 2013; 8(5): 155–160. (in Chinese)
- [12] Verrelst J, Dethier S, Rivera J P, Munoz-Mari J, Camps-Valls G, Moreno J. Active learning methods for efficient hybrid biophysical variable retrieval. *IEEE Geoscience and Remote Sensing Letters*, 2016; 13(6): 1012–1016.
- [13] Verrelst J, Rivera J P, Moreno J. ARTMO's global sensitivity analysis (GSA) toolbox to quantify driving variables of leaf and canopy radiative transfer models. *EARSel eProceedings, Special Issue 2: 9th EARSel Imaging Spectroscopy Workshop*, 2015; pp.1-11
- [14] Verrelst J, Rivera J P, van der Tol C, Magnani F, Mohammed G, Moreno J. Global sensitivity analysis of the SCOPE model: What drives simulated canopy-leaving sun-induced fluorescence. *Remote Sensing of Environment*, 2016; 166(6): 8-21.
- [15] Li X, Yu B, Xin L, Min T, Shi H. Canopy NDVI analysis and yield estimation for cotton in different nitrogen treatments. *Transactions of the CSAM*, 2014; 45(7): 231–236. (in Chinese)
- [16] Yang Y J. It is possible for unmanned aerial vehicle (UAV) fly into the billions of markets. *Chinese Pesticide*, 2015; 12: 48–55. (in Chinese)
- [17] Yasin Z M, Rahman T K A, Zakaria Z. Optimal least squares support vector machines parameter selection in predicting the output of distributed generation. *IEEE*, 2014: 152–157.
- [18] Luo X W. Thoughts on speeding up the development of agricultural aviation technology in China. *Agriculture Technology & Equipment*, 2014; 5: 7–15. (in Chinese)
- [19] Hunt E R, Doraiswamy P C, McMurtrey J E, Daughtry C S T, Perry E M, Akhmedov B. A visible band index for remote sensing leaf chlorophyll content at the canopy scale. *International Journal of Applied Earth Observation & Geoinformation*, 2013; 21(4): 103–112
- [20] Hirooka Y, Homma K, Maki M, Sekiguchi K. Applicability of synthetic aperture radar (SAR) to evaluate leaf area index (LAI) and its growth rate of rice in farmers' fields in Lao PDR. *Field Crops Research*, 2015; 176: 119–122.
- [21] Liu C G, Wang Y J, Pan K W, Jin Y Q, Jin L, Li W, et al. Photosynthetic carbon and nitrogen metabolism and the relationship between their metabolites and lipid peroxidation in dwarf bamboo (*Fargesia rufa* Yi) during drought and subsequent recovery. *Trees*, 2015; 29(6): 1–15.
- [22] Rivera J P, Verrelst J, Leoneko G, Moreno J. Multiple cost functions and regularization options for improved retrieval of leaf chlorophyll content and LAI through inversion of the PROSAIL model. *Remote Sensing*, 2013; 5(7): 3280–3304.
- [23] Mulla D J. Twenty five years of remote sensing in precision agriculture: Key advances and remaining knowledge gaps. *Biosyst. Eng.*, 2013; 114(4): 358–371.
- [24] Piekarczyk J. Application of remote sensing in agriculture. *Geoinformatica Polonica*, 2014; 13(1): 69–75.
- [25] Huang Y, Lee M A, Thomson S J, Reddy K N. Ground-based hyperspectral remote sensing for weed management in crop production. *Int J Agric & Biol Eng*, 2016; 9(2): 98–109.